Development of a Wearable IMU System for Automatically Assessing Lifting Risk Factors

Ming-Lun Lu[1(✉)], Menekse S. Barim[1], Shuo Feng[2], Grant Hughes[2], Marie Hayden[1], and Dwight Werren[1]

[1] National Institute for Occupational Safety and Health, Cincinnati, OH, USA
uzl5@cdc.gov
[2] FocusMotion, Focus Ventures Inc., Santa Monica, CA, USA

Abstract. The objective of this study was to develop a five inertial measurement unit (IMU) sensor system attached to the human body for automatically identifying the duration of the lifting task (LD) performed symmetrically with two hands at various hand locations relative to the body, and three other lifting risk variables including the trunk flexion angle (T), the vertical distance (V) and horizontal distance (H) of the lifting task defined by the revised National Institute for Occupational Safety and Health lifting equation (RNLE). The algorithm that processed the IMU data consisted of two modules: the synchronization module that extracted the synchronization feature of wrists' motion data to identify the lifting event; and the lifting variable calculations module that employed a body segment length ratio model for calculating the risk variables. The variable calculation module was further modified to include subjects' body segment length information for improved accuracy. The wearable system was validated by motion data collected by a laboratory grade motion capture system on 10 human subjects performing 360 lifting trials. Results showed that the model performed well for determining the LD ($\sim$1 s error) and T ($\sim$2° error). However, the mean errors for V and H were large (33 and 6.5 cm, respectively). Inclusion of subjects' five body segment length measurements improved the mean errors of V and H to 14 and 2.2 cm, respectively.

Keywords: IMU · Lifting · Ergonomic assessment

1 Introduction

1.1 Background

Musculoskeletal disorders (MSDs) are a major workplace health problem and economic burden. Recent data showed that workplace overexertion injuries were estimated to cost $15.1 billion a year, accounting for about 25% of the total workers' compensation cost [1]. Low back disorders (LBDs) are the largest contributor to the total workers' compensation cost. The total health care expenditures incurred by individuals with low back pain alone in the United States reached $90.7 billion a year [2].

V. G. Duffy (Ed.): HCII 2020, LNCS 12198, pp. 194–213, 2020.
https://doi.org/10.1007/978-3-030-49904-4_15

To control and prevent MSDs in the workplace, accurate quantifications of risk factors are imperative. Substantial evidence has shown that work-related physical risk factors are the main source of LBDs [3–5]. These physical risk factors include heavy/repetitive manual lifting, awkward posture, and long work hours. Combinations of these physical risk factors may lead to an increasing risk of developing LBDs [6]. Reductions of work-related physical risk factors have been the main goal of ergonomic interventions. To assess the physical risk factors for LBDs, ergonomic checklists or video task analyses are commonly used by practitioners. However, these observational risk assessment methods with the primary goal of quantifying postural risks are subjective, resource intensive; and cannot effectively quantify a variety of postures used by the worker during an 8-h workday [7, 8].

1.2 Trend in the Use of IMU for Ergonomic Assessments

Direct-reading measurements of postural risk exposures were developed by several researchers in the 90's [9–12]. However, the complex and bulky set ups did not seem to be an attractive option for field applications. With the advent of the small, wearable and light weight features of inertial measurement unit (IMU) sensors, the IMU-based ergonomic assessments are becoming a new method for tracking postural risks [13]. Many recent studies utilizing IMU sensors for ergonomic research have developed useful algorithms for measuring body postural angles, primarily the trunk flexion angle [13–15].

An IMU combines information obtained from multiple electromechanical sensors (e.g., accelerometers, gyroscopes and magnetometers) to estimate the dynamic human body motions [16]. The application of IMUs for tracking human motion as a part of the ergonomic assessment is becoming popular because the collection of the human body motion does not greatly interrupt with workers' job performance [13, 17].

Using IMU sensors for ergonomic assessments is a growing research area. Research over the past 10 years has mainly focused on the accuracy and validation of these sensor technologies. A literature search was performed using the Web of Science and Scopus databases. Records identified through the databases with the search term "ergonomic assessment" showed more than 7000 articles. The number of the articles was reduced to 450 using additional keyword search terms "inertial measurement unit" or "wearable sensor". Of 450 articles, 42 were identified manually by the authors of this study to have a research topic related to estimating joint kinematics. These selected 42 studies include various research topics of estimating joint kinematics of: the upper arm/shoulder [18–29], the cervical spine [30–32], the lower extremity [33–40], the trunk [13–15, 41–49], the whole body [13, 17, 50–53] and hand movement [54]. The majority (60%) of the literature had a focus on estimating the whole body posture and trunk movements.

1.3 Physical Risk Factors for LBDs

Manual repetitive lifting has been identified by many studies as one of the main risk factors for MSDs [3, 4]. NIOSH has identified several task variables for manual lifting that are associated with increased risks of LBDs [55]. These task variables are

summarized in the NIOSH Applications Manual for the RNLE [56]. The manual provides detailed information on the definitions of the task variables as well as the measuring methods for them.

Some of the previous studies have developed useful algorithms for measuring body postural angles, such as the trunk flexion angle [57–59]. However, these algorithms for processing data from IMU sensors have not been developed for identifying other lifting risk factors defined by the RNLE [56]. Therefore, the task variables of interest in this study were the duration of a lifting task (LD), the vertical distance between the load and the floor (V) and the horizontal distance (H) between the load and the center of the two ankles. The identification of these lifting task variables and lifting physical risk factors using IMU sensors provides valuable risk information for interventions.

1.4 Purpose of the Study

Generally, the accuracy of the wearable ensemble of sensors in measuring the body posture is a function of the number of sensors used. Detailed whole-body biomechanical models for tracking accurate body motion typically require 13 to 17 IMU sensors mounted on various body segments. For example, a commercially popular IMU-based body tracking system Xsens MVN requires wearing a body suit with 17 IMUs [60]. In our opinion, the high cost, the lengthy setup time and required expertise for using the software programs for analyzing the IMU data present a challenge for adoption in the field. One previous study [61] has shown that a five IMU sensor configuration may adequately reconstruct the whole-body posture to discriminate gross movement activities. The previous study inspired the researchers to examine the feasibility of using such a simpler system to increase the adoption of the wearable technology. In short, the purpose of this study was to assess the feasibility of using a five IMU-based wearable sensor system for automatically measuring multiple physical risk factors associated with two-handed manual lifting.

2 Methods

2.1 Design of the Five-Sensor Wearable System

Five IMU sensors (Kinetic Inc.) were attached to the subject's specific body landmarks, as shown in Fig. 1. These IMU sensors were attached to the wrists, right upper arm, upper back, and right thigh. To process data from the sensors, we used a hybrid model that incorporated machine learning and trigonometric functions for detecting lofting motion and the location of the hands in relation to the body. The input of the model was 6-axial IMU data (accelerometer and gyroscope in 3 axes respectively) sampling at 25 Hz from each of the sensors. The data were fed into two major modules including the lifting detection module and the sensor fusion module that ran in parallel. The lifting detection module detected the occurrence of a lifting event with the timestamps of the beginning (BOL) and the ending (EOL) of the event. The sensor fusion module kept track of the device orientations in real time at 25 Hz and provided the angles of the sensors in three dimensions relative to the ground. The sensor fusion model was

primarily used for correcting the gyroscope data for estimating the orientations of the body segments during a dynamic workplace environment.

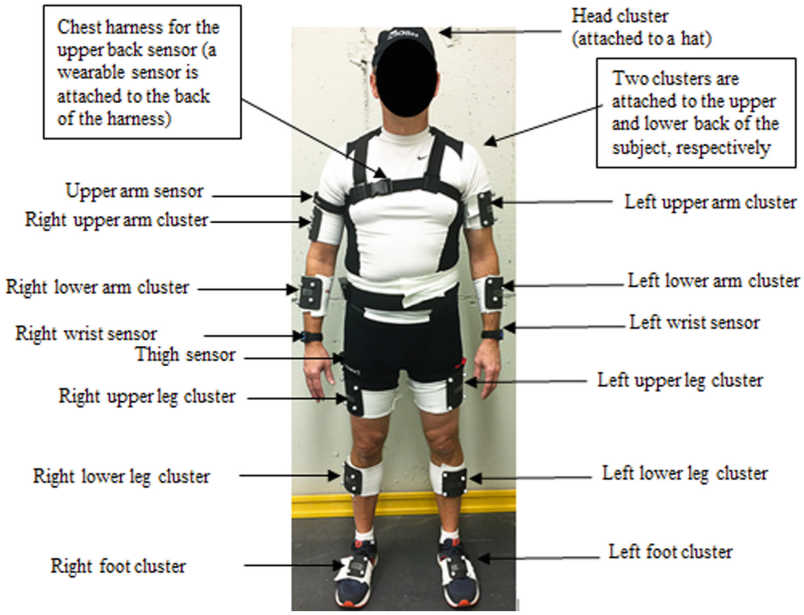

Fig. 1. Locations for five IMU sensors (one sensor located on the T12 region on the upper back is not visible) [Photo credit: CDC/NIOSH].

2.2 Lifting Risk Variables

To determine physical risk factors associated with two-handed manual lifting, the BOL and EOL were required to be identified first. Once the two time instants were determined, lifting risk factors during the lifting duration could be estimated with the lifting detection module. Three main lifting task variables used in this study were trunk flexion angle, V and H. The V and H variables were defined by the RNLE and used by the American Conference of Governmental Industrial Hygienists Threshold Limit Values (TLVs) for lifting.

2.3 Lifting Detection Module

The detection of the BOL and EOL was executed by a two-layer algorithm. The lower layer used data from two wrist sensors as input to check the motion synchronization feature of the two wrists during lifting; and outputted a binary result of the onset of synchronization and no synchronization. The higher layer or representative motion detection was a digital signal processing (DSP) layer that monitored certain events that had high correlations with the features of lifting, such as bending over and reaching out with arms. This layer ran only when the lower layer detected synchronization.

Synchronization Feature of Wrist Sensor Data. The lifting detection module constantly monitored motions (i.e., acceleration and rotation) of the two wrist sensors and determined the level of synchronization of their motions. We assumed that the two wrist sensors had high levels of synchronized motion when an object was held and moved by both hands. This assumption was based on the property of a non-elastic lifting objective that coupled the accelerations and rotations of the wrist sensors.

Machine Learning Algorithm. We used a machine learning approach to build the lifting detection module. Motion data were collected on 6 subjects performing two categories of activities: 1) performing common activities while holding a rigid box and 2) performing common activities without holding a rigid box. More specifically, for the holding-box activities, subjects performed activities of walking, turning around, raising and lowering arms while holding a rigid box for 30 s each. For the arm free activities, subjects repeated the above activities without holding the rigid box. The total data collection times for activities (1) and (2) were about 5 and 15 min, respectively. A typical sliding window approach [62–65] with a window of 2.5 s and a 0.5 s overlap was employed. For each window, IMU data from both wrist sensors were used to extract features which best represented synchronization of the wrist motions. A binary classification model was trained using a random forest classification algorithm [66]. Open source languages R and Python/C++ random forest tools were used for programming the algorithm. The binary training labels were prior-known from one of the two categories of activities. This approach was used to detect whether the two wrists were in synchronization at a 0.5 s step size over a 2.5 s long window. Namely, a decision was made based on previous 2.5 s data and updated every 0.5 s. The ratio of training and validation datasets is 5:1, resulting in a use of 25 min of hands synchronized data for training and 5 min of data for validation. This module achieved a training accuracy of 83%–85% detection rate, and about 32% in false alarm rate [67].

Representative Motion Detection. The motion detection layer or the higher layer was necessary in that the lower layer only provided a binary decision over a 2.5 s window without providing the exact starting and ending moment of a lifting event. This module was aimed to detect certain events that were highly likely to happen during lifting events by tracking the motion data of certain body parts. Sample motions included: extending arms out together, bending over and turning around in whole body motion. Each of these motions are extracted from sensor data of corresponding body parts as a one dimensional signal. The signal had peaks at the moment of these events. These signals were combined together to amplify the signature event. The exact moment of BOL and EOL were then available using the peaks of the combined signal. This higher layer only ran when the lower layer detected the motion synchronization feature of the two wrists. The lower layer remained idle when both wrists were not in synchronization, such as walking.

2.4 Sensor Fusion Module

IMU sensors typically measure three-dimensional data from accelerometer and gyroscope sensors. The accelerometer sensor, measuring three-dimensional linear acceleration, produces a vector sum of the acceleration caused by gravity and the acceleration

caused by motion. The gravity acceleration provides the device orientation information if it can be isolated from the sum. The gyroscope measures the three-dimensional angular velocity (i.e., rotation rate) [68, 69], and the track of history indicates the changes of device orientation. However, the track has to be done by an integral from angular rate to angles, which generates a large accumulative drift [70]. An extended Kalman filter algorithm, similar to that used by Rigatos and Tzafestas [71] was used to fuse the accelerometer and gyroscope data of a single device and then output gravity vector information (from accelerometer data) with motion induced acceleration and bias of gyroscope data attenuated. This gravity vector provided information of device orientation in real time for improving the identification of the lifting event.

2.5 Calculations of Trunk Flexion Angle, V and H

This sensor fusion was applied to all the individual sensors prior to the calculations of the lifting risk variables. The trunk flexion angle was directly available from gyroscope data from the upper back sensor placed on the T12 region of the spine. A calibration for the trunk flexion angle was performed to account for the natural lordosis of the spine while standing upright. This means that the trunk flexion angle was calibrated by subtracting the slight angle from the line of gravity using the data collected during quiet upright standing.

As shown in Fig. 2, the angular data of four sensors (Q_{UA}, Q_{FA}, Q_{back}, Q_{thigh}) were input into the equations below for calculating V and H. Because of the redundant information of the synchronized wrist motion, data from the left wrist sensor was ignored in calculating the two variables. Because subjects did not significantly flex the lower legs during the lifting tasks, the Q_{calf} angle during lifts was assumed to have little effect on the calculations of the lifting risk variables. Therefore, the Q_{calf} angle was not input into the equations.

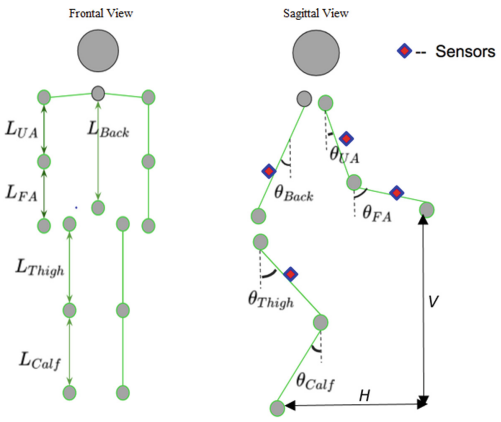

Fig. 2. Body length ratio model and angular data of four sensors used for estimating V and H.

$$V = L_{back} \times \cos(\theta_{Back}) + L_{Thigh} \times \cos(\theta_{Thigh}) + L_{calf} - L_{UA} \times \cos(\theta_{UA}) - L_{FA} \times \cos(\theta_{FA})$$

$$H = L_{UA} \times \sin(\theta_{UA}) + L_{FA} \times \sin(\theta_{FA}) + L_{Back} \times \sin(\theta_{Back}) - L_{thigh} \times \sin(\theta_{Thigh})$$

The variable calculation module was based on a body length ratio model using the right forearm length as the basic unit to estimate the lengths of other body segments. Based on population anthropomorphic data, the length of the upper arm (L_{UA}) approximated the length of the forearm (L_{FA}); the length of the upper leg (L_{Thigh}) or the lower leg (L_{Calf}) approximated 1.2 times L_{FA}; and the length of the spine (L_{back}) was estimated to be 1.4 times L_{FA}. This body length ratio model simplified the data collection process without a need for measuring the lengths of various body segments.

Because the calculations of V and H were based on the actual measurement of the forearm length, the body length ratio model was able to compute V and H as distances. To improve the accuracy of the variable calculations method, it was revised to include input of subjects' specific anthropometric measurements of forearm length, upper arm length, back length, thigh length and calf length. In this paper, we used the terms "ratio" and "ratio + length" as the first and second models, respectively.

2.6 Validation of the Algorithm for Measuring the Lifting Risk Variables

Human Subjects. Ten subjects (five males and five females) in NIOSH, Cincinnati, Ohio, volunteered to participate in the study. The subjects' mean and SD for age, statue and weight were 51.50 ± 9.83 years; 170 ± 7.4 cm and 85.7 ± 20.2 kg, respectively. Prior to data collection, written consents were obtained from the subjects in accordance with NIOSH's Internal Review Board's approved study protocol.

Instrumentation and Data Collection. Subjects' motion data were collected in a laboratory environment with the five wearable IMU sensor system and a motion capture system (OptiTrack, NaturakPoint Inc. and the MotionMonitor® system, Innovative Sports Inc.). During data collection, the IMU data were streamed continuously from 5 sensors to a data logger at a rate of 25 samples per second through Bluetooth connection. Prior to data collection, the internal clock of the sensor data logger was synchronized with the universal time clock (UTC), which was used to synchronize the motion capture data and the videos recorded by a Microsoft web camera at a resolution of 480p. The camera viewing angle was approximately perpendicular to the subjects' sagittal plane.

Subjects were asked to perform symmetrical lifting tasks to produce commonly used body postures for 12 lifting zones defined by the ACGIH TLVs for lifting classification (Fig. 3). The definitions of the V and H originated from the RNLE. Basically, these lifting zones were defined by the combination of H and V for symmetrical lifting on the sagittal plane. The midpoints of the lifting zones were used as the positions for starting the lifting tasks, except for zones 1–3, 4, 7, and 10. The alternative starting locations of the lifting tasks for the exceptional zones were chosen for realistic lifting motion within subjects' reach distances. Each task was repeated three times for a total

36 lifting trials for each subject. The initial lifting positions were adjusted according to each subject's anthropometric information. These trials were assigned to each subject in random order to reduce learning effects.

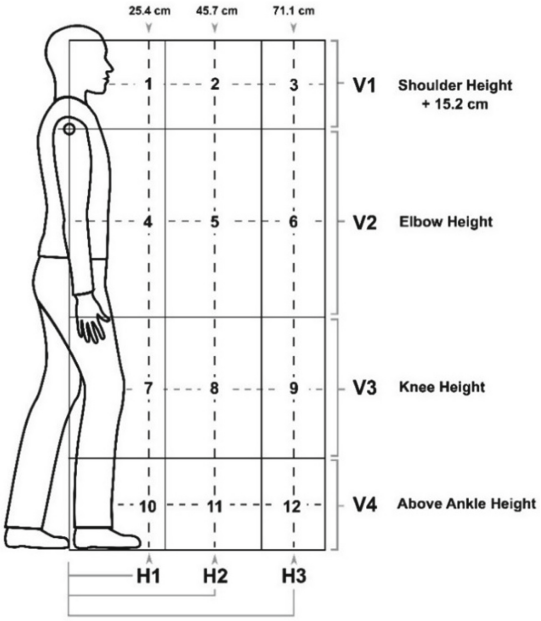

Fig. 3. Initial lifting positions based on the ACGIH TLV for lifting (H1: Near horizontal distance from the basket, H2: Middle distance, H3: Far distance, V1: Vertical height shoulder level, V2: Waist level, V3: Knee level and V4: Floor level)

A wired grid weighing about 0.45 kg and measuring 36 × 12 cm in size with two cutout handles was used to simulate lifting a tote box during the trials. The grid was designed to help subjects create a realistic lifting motion while minimizing obstructions for body motion measurements by the optical motion capture system. A small platform (12 × 12 cm) was used to hold the grid for setting the initial lifting height. A shelf (77.5 cm in height) as the ending position of the lifting trials was set up opposite of the initial lifting location. The distance between the initial and ending positions of the lifting trials was 3.4 m.

Before each trial, three distances of H were marked on the floor to guide the subjects to lift from one of the designated zones classified by H (25.4, 45.7 and 71 cm from the center of the two ankles to the center of the grid). With the pre-determined locations of the feet and hands in the zones, the lifting postures from the 12 zones were assured.

Identification of BOL and EOL. Video recordings from the motion capture system were used to manually identify the beginning and ending of each lifting trial. Two NIOSH researchers reviewed the video recordings to identify the video frame

numbers for the BOL and the EOL for each trial. The criteria for determining the frame numbers were based on the moment when the grid started to move for the BOL and the moment when the grid was set down completely by two hands for the EOL.

Data Analysis. Because the 12 lifting zones were set up at the BOL, the V, H, and trunk flexion (T) at the BOL were determined by the motion capture system and used as the gold standard for determining the accuracy of the algorithm. The motion capture system calculated V, H and T using matrix and trigonometric functions applied to body segment and joint center data estimated from the marker clusters in Fig. 1 [8, 72]. The arithmetic difference in the timestamps identified by the algorithm and the observation method was used as the error measure for lifting duration. The mean of this error measure was calculated across all subjects by the lifting zone to evaluate different error levels as a function of the lifting zone. The measurements of V, H and trunk flexion angle between the wearable system and the motion capture system were compared using the Bland-Altman plots. The plots were made for the ratio and ratio + length models respectively.

3 Results

3.1 Accuracy of Lifting Duration Measurements

Table 1 shows the accuracy levels of LD (EOL − BOL) measured by the IMU system for the 12 lifting zones. The average accuracy level for the lifting zones was about one sec (0.939 s), with the largest error 1.079 s for the zone 12 and the smallest 0.622 s for the zone 5. There was about a one-second systematical delay in identifying BOL and EOL for each lifting trial by the algorithm. The input of additional body segment length data did not affect the estimation of the lifting duration.

Table 1. Lifting duration differences between the wearable IMU and motion capture systems (lifting zone number is presented in the parentheses)

Lifting duration differences (sec) Average ± SD		
Total difference within all subjects and zones is 0.939 ± 0.673		
(1) 1.056 ± 0.586	(2) 1.036 ± 0.596	(3) 0.949 ± 0.705
(4) 0.879 ± 0.820	(5) 0.622 ± 0.386	(6) 0.754 ± 0.528
(7) 1.052 ± 1.029	(8) 1.032 ± 0.976	(9) 0.913 ± 0.466
(10) 0.884 ± 0.548	(11) 1.014 ± 0.493	(12) 1.079 ± 0.565

3.2 Accuracy of V Measurements

Figure 4 shows the Bland-Altman plots for comparing the V variable measured by the ratio model of the wearable system and the motion capture system. In the Bland-Altman plot, the Y axis represents the difference in V measured by the two systems

(Vw: wearable system; Vm: motion capture system), whereas the X axis represents the mean value of V measured by the two systems. The mean of the differences in all measurements represents the bias or error of the wearable system. The lower and upper levels of agreement (LOA) represent the 95% confidence interval (±1.96 SD) of the mean difference. Negative and positive signs of the differences or errors on the Y axis indicate under- and over-estimation of the wearable system. As shown in Fig. 7, the mean error (Vw-Vm) of all the measurements was −33 cm. The mean errors of V for the four vertical zones V_1–V_4 were −43, −30, −28 and −31 cm, respectively. The scattered data points of the wearable system for the vertical zone V_3 crosses 0 difference (i.e., 100% matched with the motion capture data), indicating an increased accuracy level for measuring V between the knuckle and mid-shin heights.

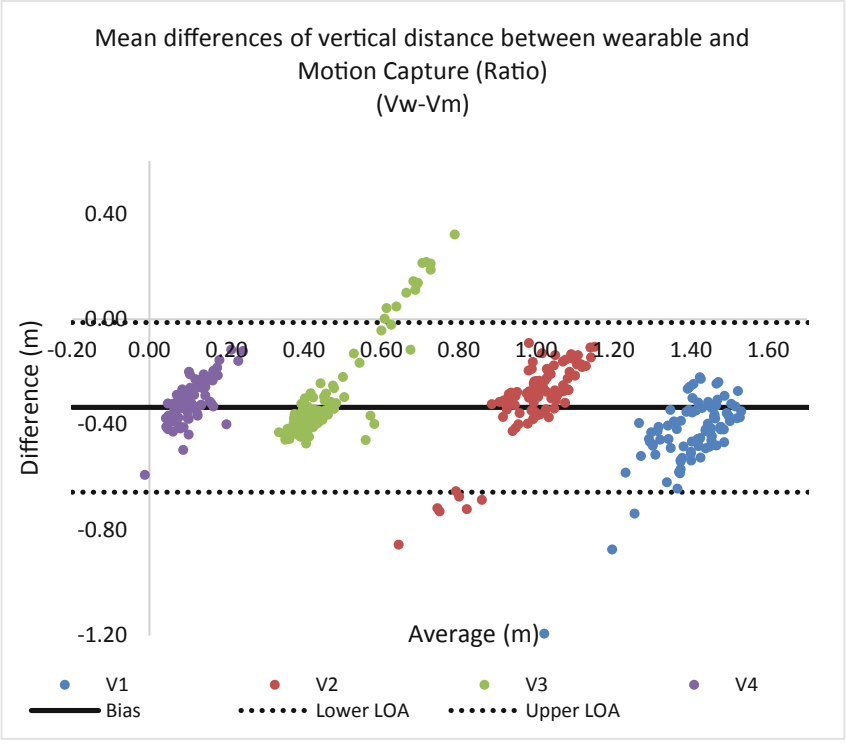

Fig. 4. The Bland-Altman plot for comparing V measured by the ratio model of the wearable system and the motion capture system

Figure 5 shows the Bland-Altman plots for comparing the V variable measured by the ratio + length model of the wearable system and the motion capture system. The mean error (Vw-Vm) of V measured by the wearable system was −14 cm. The mean errors of V for the four vertical zones V_1–V_4 were −14, −4, −12 and −28 cm, respectively. The scattered data points of the measurement errors for all four vertical

zones cross 0 (i.e., 100% matched with data measured by the motion capture data), indicating an improved accuracy level for measuring V for all vertical zones.

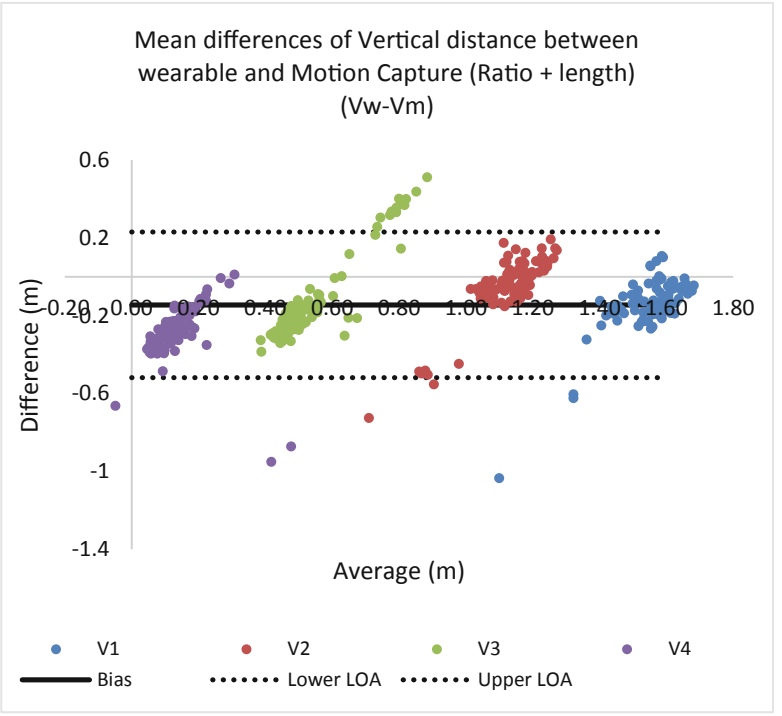

Fig. 5. The Bland-Altman plot for comparing V measured by the ratio + length model of the wearable system and the motion capture system

3.3 Accuracy of H Measurements

Figures 6 shows the Bland-Altman plots for the H variable calculated by the ratio model. The mean and SD of the error in H measured by the wearable system was −6.2 cm and 19 cm. The mean errors and SDs of H measured by the wearable system for H_1, H_2 and H_3 were −12 ± 13.5, −7 ± 13.7 and −23.5 ± 10.9 cm, respectively. The performance of the ratio model for measuring H was poor. The poor performance was significantly affected by the horizontal location of the lift deviated from the middle zones.

Figures 7 shows the Bland-Altman plots for the H variable calculated by the ratio model. The mean and SD of the error in H measured by the wearable system was −2.2 cm and 21.9 cm. The mean errors and SDs of H measured by the wearable system for H_1, H_2 and H_3 were −18 ± 16, −0.9 ± 13.7 and −19 ± 15 cm. With the input of the body segment length data, the performance of the ratio model for measuring H was improved. However, the performance was still significantly affected by the horizontal location of the lift deviated from the middle zones.

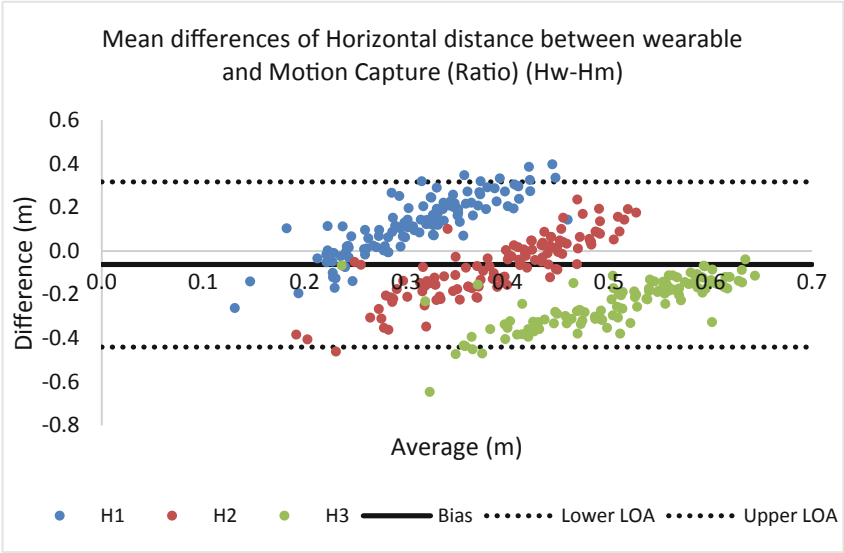

Fig. 6. The Bland-Altman plot for comparing H measured by the ratio model of the wearable system and the motion capture system

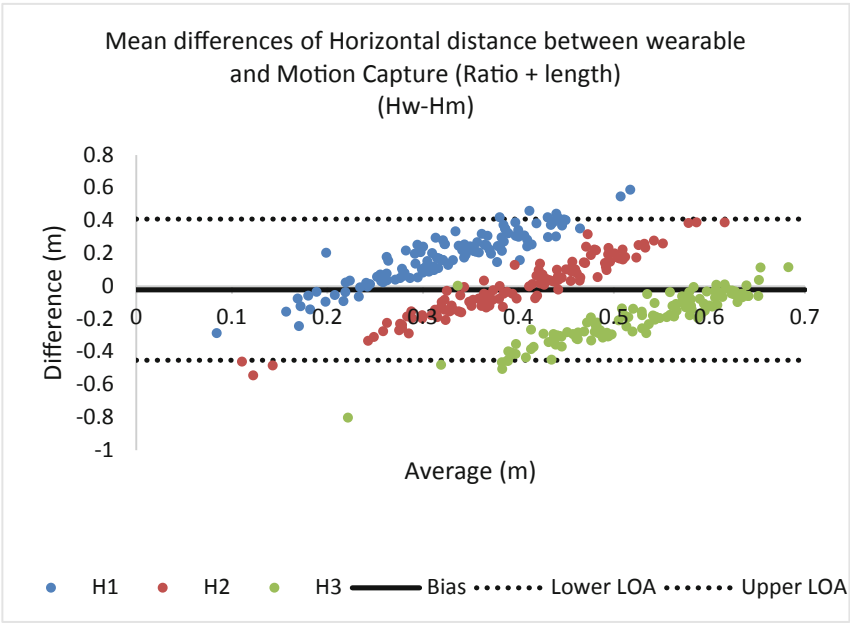

Fig. 7. The Bland-Altman plot for comparing H measured by the ratio + length model of the wearable system and the motion capture system

3.4 Accuracy of Trunk Flexion Angle (T)

The Bland-Altman plot for T is shown in Fig. 8. The mean (±SD) of T measured by the motion capture system and the wearable system were 37.5° (±32.8°) and 39.8° (±32.9), respectively. The mean error (Tw-Tm) of the wearable system across all lifting heights was −2.4°. To examine the effect of the different lifting heights on the T measurements, the mean error is presented as a function of the vertical zones (V_1, V_2, V_3 and V_4) in four different colors in Fig. 8. The mean errors for V_1 to V_4 were −2.3°, −1.6°, −7.8° and −2.5°, respectively. Similar to the lifting duration, the use of additional body segment length data did not affect the accuracy of estimating the trunk flexion angle.

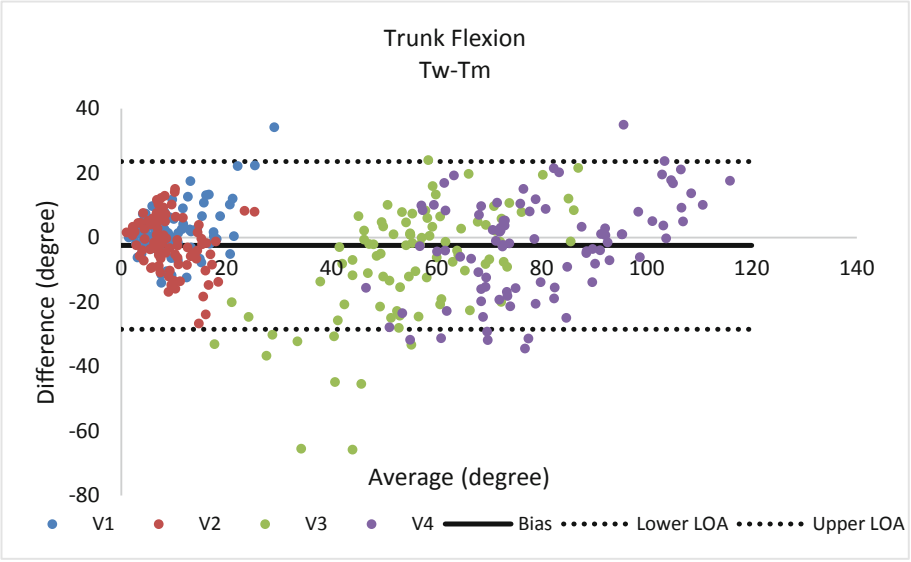

Fig. 8. The Bland-Altman plot for comparing the trunk flexion angle (T) measured by the wearable (Tw) and the motion capture (Tm) systems

4 Discussion

This paper describes the development and validation of an algorithm for processing motion data from a five IMU-based wearable sensor system attached to the human body for measuring the LD, T and various hand locations (V and H) in relation to the body at the beginning of the lift.

The study results showed that the algorithm using two wrist sensors was capable of measuring LD within approximately one second of error. Although there was a systematic delay in timestamping both BOL and EOL, the large differences in LD between the two motion measuring systems were primarily caused by increased differences in the measurements for estimating the timestamps for EOL. The two analysts noticed that

during EOL, many subjects may have turned their torso while releasing the grid. This inconsistent lifting behavior may have caused the increased differences in the identification of EOL between the two motion measuring systems.

The body segment length ratio model using the gyroscope data relative to the gravity direction did not perform well in measuring V and H. The poor performance (mean errors of 33 and 6.5 cm for V and H, respectively) of the model was caused by two main factors. First, a small change in the body segment ratio may result in a large measurement in the simplistic body segment ratio model. A precise measurement of the body segments improved the performance of the equations, as shown in the reduced mean errors of (6.2 and 2.2 cm for V and H, respectively) of the ratio + length model. Second, the rotations of the sensors on the arm may have caused inaccurate angular data. The X axis of the gyroscope data relative to the gravity direction was used for calculating V. The pronation of the arms, in particular the lower arms observed during the lifting trials in the V_1 zone, changed the projection of the x axis on the sagittal plane. Consequently, the angular data of the sensors on the pronated arms might have caused inaccurate calculations of V. This finding is substantiated by the increased errors of both V and H variables in the V_1 zone. Because of the increased errors, cautions should be exercised when using both models for measuring H in the lifting zones that deviated from the middle horizontal zone.

Upon a closer review of the motion capture data of the lifting trials, we found that the lifting motion of a small percentage (7%) of the lifting trials was not even (i.e., difference in Vm of both wrists > 3 cm) during BOL. This uneven motion may have produced two effects on the study results. First, it may have caused inconsistent identifications of the frame numbers for BOL and EOL for even and uneven lifts. Second, it may have resulted in increased differences of V and H between the two motion measuring systems. The wearable system, however, could only record the movements of the right arm. Consequently, inaccurate measurements of V and H by the wearable system were anticipated due to the uneven lifting motion of both arms.

There was a small percentage (8%) of missing motion data captured by the motion capture system. Proxy data were used based on the data available within 15 frames of the frame numbers identified for BOL and EOL. We decided to use the proxy data after a careful review of the hand and foot positions that matched the position for the BOL and EOL. This manual identification of the matched body movements may have caused slight bias in the comparisons of the V and H measured by the two systems.

One of the first direct-reading instruments for mearing trunk kinematics for ergonomic assessments was the lumbar motion monitoring (LMM) developed by Marras et al. [11] using multiple three-axial electro-goniometer attached to an exoskeleton system worn by the user. In that study, the accuracy (average 1.7° error) of the LMM was determined by 20 different ranges of lifting motion. In this study, the 2° error in measuring the trunk flexion angle by one wearable IMU was similar to that in Marras et al.'s [11] study and another previous study using an IMU sensor [73].

As compared with other vertical zones, the increased error (7.8°) of this wearable IMU system in measuring the trunk flexion angle for V3 is unclear. It is speculated that the trunk flexion angels for the lifting trials in V3 were varying to a larger degree, which potentially lead to a wider spread of data and the increased average error for this zone.

The H and V variables are very critical factors for using the RNLE or the ACGIH TLV for lifting. Taking measurements for these two variables in the field, the interruption of the worker's task is inevitable. Using the proposed wearable system for measuring the variables may provide a practical solution to the challenge of field data collection. Although results from this study showed large errors in the measurements of V and H for a variety of lifting postures, the identifications of BOL, EOL, LD and T by the system may be useful.

Several limitations of the wearable system are worth mentioning. First, the body length ratio model used in this study simplifies the data collection process at a cost of reduced accuracy. Second, with the additional input of the body segment length information, the improved average accuracy levels of H and V measurements may not be adequate for measuring hand location deviating from the middle horizontal zone, above the shoulder and below mid-shin heights. Third, the algorithm cannot be applied to one-handed or two-handed lifting tasks with uneven lifting movements of the two wrists. Finally, the algorithm was not designed for any lifting tasks involving trunk rotation or lateral movements.

5 Conclusions

A five-IMU sensor system attached to the human body was developed and validated for automatically identifying the duration of the two-handed lifting tasks and three other lifting risk variables including T, V and H defined by the RNLE and the ACGIH TLV for lifting. We used a hybrid approach that incorporated a machine learning algorithm to identify the lifting event first, followed by a body segment length ratio model that computed V and H with an optional input of the body segment length information for improved accuracy. The machine learning algorithm performed well for determining the LD within one second error. The calculation of T using the gyroscope data of one sensor on the upper back was fairly accurate within 2° error. However, the body segment length ratio model did not produce robust accuracy levels for V and H, even with additional input of body segment length information. Some of the findings from this study may be used for designing an IMU-based instrument for real-time risk monitoring of two-handed lifting activities in the workplace.

Acknowledgements and Disclaimer. The study was financially supported by intramural funding from the National Institute for Occupational Safety and Health (NIOSH). No conflict of interest is declared. This project was supported in part by an appointment to the Research Participation Program at the Centers for Disease Control and Prevention administered by the Oak Ridge Institute for Science and Education through an interagency agreement between the U.S. Department of Energy and the Centers for Disease Control and Prevention. Disclaimer: The findings and conclusions in this article are those of the authors and do not necessarily represent the official position of the National Institute for Occupational Safety and Health, Centers for Disease Control and Prevention.

References

1. Liberty Mutual Research Institute for Safety: Liberty Mutual Workplace Safety Index. Liberty Mutual 175 Berkeley St., Boston, MA 02116 (2014)
2. Luo, X., Pietrobon, R., Sun, S.X., Liu, G.G., Hey, L.: Estimates and patterns of direct health care expenditures among individuals with back pain in the United States. Spine **29**(1), 79–86 (2004)
3. Bernard, B.P.: Musculoskeletal Disorders and Workplace Factors: A Critical Review of Epidemiologic Evidence for Work-Related Musculoskeletal Disorders of the Neck, Upper Extremity, and Low Back. U.S. Department of Health and Human Services, Center for Disease Control and Prevention, National Institute for Occupational Health and Safety, Cincinnati OH (1997)
4. National Research Council: Musculoskeletal Disorders and the Workplace: Low Back and Upper Extremities, Washington, DC (2001)
5. da Costa, B.R., Vieira, E.R.: Risk factors for work-related musculoskeletal disorders: a systematic review of recent longitudinal studies. Am. J. Ind. Med. **53**(3), 285–323 (2010)
6. Lu, M.L., Waters, T.R., Krieg, E., Werren, D.: Efficacy of the revised NIOSH lifting equation to predict risk of low-back pain associated with manual lifting: a one-year prospective study. Hum. Factors **56**(1), 73–85 (2014)
7. Callaghan, J.P., Salewytsch, A.J., Andrews, D.M.: An evaluation of predictive methods for estimating cumulative spinal loading. Ergonomics **44**(9), 825–837 (2001)
8. Lu, M.L., Waters, T., Werren, D.: Development of human posture simulation method for assessing posture angles and spinal loads. Hum. Factors Ergon. Manuf. Serv. Ind. **25**(1), 123–136 (2015)
9. Radwin, R.G., Lin, M.L.: An analytical method for characterizing repetitive motion and postural stress using spectral-analysis. Ergonomics **36**(4), 379–389 (1993)
10. Bhattacharya, A., Warren, J., Teuschler, J., Dimov, M., Medvedovic, M., Lemasters, G.: Development and evaluation of a microprocessor-based ergonomic dosimeter for evaluating carpentry tasks. Appl. Ergon. **30**(6), 543–553 (1999)
11. Marras, W.S., Fathallah, F.A., Miller, R.J., Davis, S.W., Mirka, G.A.: Accuracy of a three-dimensional lumbar motion monitor for recording dynamic trunk motion characteristics. Int. J. Ind. Ergon. **9**(1), 75–87 (1992)
12. Freivalds, A., Kong, Y., You, H., Park, S.: A comprehensive risk assessment model for work-related musculoskeletal disorders of the upper extremities. In: Proceedings of Human Factors and Ergonomics Society Annual Meeting, vol. 44, no. 31, pp. 5-728–5-731. SAGE Publications, Los Angeles (2000)
13. Battini, D., Persona, A., Sgarbossa, F.: Innovative real-time system to integrate ergonomic evaluations into warehouse design and management. Comput. Ind. Eng. **77**, 1–10 (2014)
14. He, Z., Jin, L.: Activity recognition from acceleration data based on discrete cosine transform and SVM. In: 2009 IEEE International Conference on Systems, Man and Cybernetics, San Antonio TX, pp. 5041–5044. IEEE (2009)
15. Dahlqvist, C., Hansson, G.Å., Forsman, M.: Validity of a small low-cost triaxial accelerometer with integrated logger for uncomplicated measurements of postures and movements of head, upper back and upper arms. Appl. Ergon. **55**, 108–116 (2016)
16. Schall Jr., M.C., Fethke, N.B., Chen, H., Oyama, S., Douphrate, D.I.: Accuracy and repeatability of an inertial measurement unit system for field-based occupational studies. Ergonomics **59**(4), 591–602 (2015)

17. Brents, C., Hischke, M., Reiser, R., Rosecrance, J.: Low back biomechanics of keg handling using inertial measurement units. In: Bagnara, S., Tartaglia, R., Albolino, S., Alexander, T., Fujita, Y. (eds.) IEA 2018. AISC, vol. 825, pp. 71–81. Springer, Cham (2019). https://doi.org/10.1007/978-3-319-96068-5_8
18. Zhou, H., Hu, H., Tao, Y.: Inertial measurements of upper limb motion. Med. Biol. Eng. Comput. **44**(6), 479–487 (2006)
19. Zhou, H., Stone, T., Hu, H., Harris, N.: Use of multiple wearable inertial sensors in upper limb motion tracking. Med. Eng. Phys. **30**(1), 123–133 (2008)
20. Zhou, H., Hu, H.: Reducing drifts in the inertial measurements of wrist and elbow positions. IEEE Trans. Instrum. Meas. **59**(3), 575–585 (2010)
21. Zhou, H., Hu, H.: Upper limb motion estimation from inertial measurements. Int. J. Inf. Technol. **13**(1), 1–14 (2007)
22. Cutti, A.G., Giovanardi, A., Rocchi, L., Davalli, A., Sacchetti, R.: Ambulatory measurement of shoulder and elbow kinematics through inertial and magnetic sensors. Med. Biol. Eng. Comput. **46**(2), 169–178 (2008)
23. de Vries, W., Veeger, H., Cutti, A., Baten, C., van der Helm, F.: Functionally interpretable local coordinate systems for the upper extremity using inertial & magnetic measurement systems. J. Biomech. **43**(10), 1983–1988 (2010)
24. El-Gohary, M., McNames, J.: Shoulder and elbow joint angle tracking with inertial sensors. IEEE Trans. Biomed. Eng. **59**(9), 2635–2641 (2012)
25. Vignais, N., Miezal, M., Bleser, G., Mura, K., Gorecky, D., Marin, F.: Innovative system for real-time ergonomic feedback in industrial manufacturing. Appl. Ergon. **44**(4), 566–574 (2013)
26. Caputo, F., D'Amato, E., Spada, S., Sessa, F., Losardo, M.: Upper body motion tracking system with inertial sensors for ergonomic issues in industrial environments. In: Goonetilleke, R., Karwowski, W. (eds.) Advances in Physical Ergonomics and Human Factors. AISC, vol. 489, pp. 801–812. Springer, Cham (2016). https://doi.org/10.1007/978-3-319-41694-6_77
27. Morrow, M.B., Lowndes, B., Fortune, E., Kaufman, K.R., Hallbeck, M.: Validation of inertial measurement units for upper body kinematics. J. Appl. Biomech. **33**(3), 227–232 (2017)
28. Chen, H., Schall Jr., M.C., Fethke, N.: Accuracy of angular displacements and velocities from inertial-based inclinometers. Appl. Ergon. **67**, 151–161 (2018)
29. Peppoloni, L., Filippeschi, A., Ruffaldi, E., Avizzano, C.A.: A novel 7 degrees of freedom model for upper limb kinematic reconstruction based on wearable sensors. In: 2013 IEEE 11th International Symposium on Intelligent Systems and Informatics, Subotica Serbia, pp. 105–110. IEEE (2013)
30. Jasiewicz, J.M., Treleaven, J., Condie, P., Jull, G.: Wireless orientation sensors: their suitability to measure head movement for neck pain assessment. Manual Ther. **12**(4), 380–385 (2007)
31. Theobald, P.S., Jones, M.D., Williams, J.M.: Do inertial sensors represent a viable method to reliably measure cervical spine range of motion? Manual Ther. **17**(1), 92–96 (2012)
32. Duc, C., Salvia, P., Lubansu, A., Feipel, V., Aminian, K.: A wearable inertial system to assess the cervical spine mobility: comparison with an optoelectronic-based motion capture evaluation. Med. Eng. Phys. **36**(1), 49–56 (2014)
33. Favre, J., Jolles, B.M., Aissaoui, R., Aminian, K.: Ambulatory measurement of 3D knee joint angle. J. Biomech. **41**(5), 1029–1035 (2008)
34. Picerno, P., Cereatti, A., Cappozzo, A.: Joint kinematics estimate using wearable inertial and magnetic sensing modules. Gait Posture **28**(4), 588–595 (2008)

35. Ferrari, A., et al.: First in vivo assessment of "Outwalk": a novel protocol for clinical gait analysis based on inertial and magnetic sensors. Med. Biol. Eng. Comput. **48**(1), 1–15 (2010)
36. Fong, D.T., Chan, Y.Y.: The use of wearable inertial motion sensors in human lower limb biomechanics studies: a systematic review. Sensors **10**(12), 11556–11565 (2010)
37. Bolink, S.A.A.N., et al.: Validity of an inertial measurement unit to assess pelvic orientation angles during gait, sit-stand transfers and set-up transfers: comparison with an optoelectronic motion capture system. Med. Eng. Phys. **38**(3), 225–231 (2016)
38. Beravs, T., Rebersek, P., Novak, D., Podobnik, J., Munih, M.: Development and validation of a wearable inertial measurement system for use with lower limb exoskeletons. In: 2011 11th IEEE-RAS International Conference on Humanoid Robots, Bled Slovenia, pp. 212–217. IEEE (2011)
39. O'Reilly, M.A., Whelan, D.F., Ward, T.E., Delahunt, E., Caulfield, B.: Classification of lunge biomechanics with multiple and individual inertial measurement units. Sports Biomech. **16**(3), 342–360 (2016)
40. Teufl, W., Miezal, M., Taetz, B., Frohlich, M., Bleser, G.: Validity of inertial sensor-based 3D joint kinematics of static and dynamic sport and physiotherapy specific movements. PLOS One **14**(2), 1–18 (2019)
41. Lee, R.Y.W., Laprade, J., Fung, E.H.K.: A real-time gyroscopic system for three-dimensional measurement of lumbar spine motion. Med. Eng. Phys. **25**(10), 817–824 (2003)
42. Goodvin, C., Park, E.J., Huang, K., Sakaki, K.: Development of a real-time three-dimensional spinal motion measurement system for clinical practice. Med. Biol. Eng. Comput. **44**(12), 1061–1075 (2006)
43. Giansanti, D., Maccioni, G., Benvenuti, F., Macellari, V.: Inertial measurement units furnish accurate trunk trajectory reconstruction of the sit-to-stand manoeuvre in healthy subjects. Med. Biol. Eng. Comput. **45**(10), 969–976 (2007)
44. Plamondon, A., et al.: Evaluation of a hybrid system for three-dimensional measurement of trunk posture in motion. Appl. Ergon. **38**(6), 697–712 (2007)
45. Roetenberg, D., Slycke, P.J., Veltink, P.H.: Ambulatory position and orientation tracking fusing magnetic and inertial sensing. IEEE Trans. Biomed. Eng. **54**(5), 883–890 (2007)
46. Kim, S., Nussbaum, M.A.: Performance evaluation of a wearable inertial motion capture system for capturing physical exposures during manual material handling tasks. Ergonomics **56**(2), 314–326 (2013)
47. Bauer, C.M., et al.: Concurrent validity and reliability of a novel wireless inertial measurement system to assess trunk movement. J. Electromyogr. Kinesiol. **25**(5), 782–790 (2015)
48. Bergamini, E., Guillon, P., Camomilla, V., Pillet, H., Skalli, W., Cappozzo, A.: Trunk inclination estimate during the sprint start using an inertial measurement unit: a validation study. J. Appl. Biomech. **29**(5), 622–627 (2013)
49. Monaco, M.G.L., et al.: Biomechanical overload evaluation in manufacturing: a novel approach with sEMG and inertial motion capture integration. In: Bagnara, S., Tartaglia, R., Albolino, S., Alexander, T., Fujita, Y. (eds.) IEA 2018. AISC, vol. 818, pp. 719–726. Springer, Cham (2019). https://doi.org/10.1007/978-3-319-96098-2_88
50. Brodie, M.A., Walmsley, A., Page, W.: Dynamic accuracy of inertial measurement units during simple pendulum motion. Comput. Methods Biomech. Biomed. Eng. **11**(3), 235–242 (2008)
51. Brodie, M.A., Walmsley, A., Page, W.: Fusion motion capture: a prototype system using inertial measurement units and GPS for the biomechanical analysis of ski racing. Sports Technol. **1**(1), 17–28 (2008)

52. Robert-Lachaine, X., Mecheri, H., Larue, C., Plamondon, A.: Validation of inertial measurement units with an optoelectronic system for whole-body motion analysis. Med. Biol. Eng. Comput. **55**(4), 609–619 (2017)
53. Maurice, P., et al.: Human movement and ergonomics: an industry-oriented dataset for collaborative robotics. Int. J. Robot. Res. **38**(14), 1529–1537 (2019)
54. Nemec, D., Hrubos, M., Pirnik, R., Janota, A., Simak, V.: Ergonomic remote control of the mobile platform by inertial measurement of the hand movement. In: 2016 ELEKTRO, Strbske Pleso Slovakia, pp. 445–449. IEEE (2016)
55. Waters, T.R., Putz-Anderson, V., Garg, A., Fine, L.J.: Revised NIOSH equation for the design and evaluation of manual lifting tasks. Ergonomics **36**(7), 749–776 (1993)
56. Waters, T.R., Putz-Anderson, V., Garg, A.: Applications Manual for the Revised NIOSH Lifting Equation. U. S. Department of Health and Human Services, National Institute for Occupational Safety and Health, Cincinnati OH (1994)
57. Aoki, T., Feng-Shun Lin, J., Kulic, D., Venture, G.: Segmentation of human upper body movement using multiple IMU sensors. In: 2016 38th Annual International Conference of the IEEE Engineering in Medicine and Biology Society (EMBC), Orlando FL, USA, pp. 3163–3166. IEEE (2016)
58. Fang, Z., Yang, Z., Wang, R.-B., Chen, S.-Y.: Inertial sensor-based knee angle estimation for gait analysis using the ant colony algorithm to find the optimal parameters for Kalman filter. In: 2018 3rd International Conference on Automation, Mechanical and Electrical Engineering (AMEE 2018), pp. 249–254 (2018)
59. Seel, T., Raisch, J., Schauer, T.: IMU-Based joint angle measurement for gait analysis. Sensors **14**(4), 6891–6909 (2014)
60. Roetenberg, D., Luinge, H., Slycke, P.: Xsens MVN: full 6 DOF human motion tracking using miniature inertial sensors. Xsens Motion Technologies BV, Enschede, The Netherlands (2009)
61. Wouda, F.J., Giuberti, M., Bellusci, G., Veltink, P.H.: Estimation of full-body poses using only five inertial sensors: an eager or lazy learning approach. Sensors **16**(2), 2138 (2016)
62. Spriggs, E.H., De La Torre, F., Hebert, M.: Temporal segmentation and activity classification from first-person sensing. In: 2009 IEEE Computer Society Conference on Computer Vision and Pattern Recognition Workshops, Miami FL, USA, pp. 17–24. IEEE (2009)
63. Bulling, A., Blanke, U., Schiele, B.: A tutorial on human activity recognition using body-worn inertial sensors. ACM Comput. Surv. (CSUR) **46**(3), 1–33 (2014)
64. Moncada-Torres, A., Leuenberger, K., Gonzenbach, R., Luft, A., Gassert, R.: Activity classification based on inertial and barometric pressure sensors at different anatomical locations. Physiol. Meas. **35**(7), 1245 (2014)
65. Attal, F., Mohammed, S., Dedabrishvili, M., Chamroukhi, F., Oukhellou, L., Amirat, Y.: Physical human activity recognition using wearable sensors. Sensors **15**(12), 31314–31338 (2015)
66. Liaw, A., Wiener, M.: Classification and regression by randomForest. R News **2**(3), 18–22 (2002)
67. Powers, D.M.: Evaluation: from precision, recall and F-measure to ROC, informedness, markedness and correlation (2011)
68. Foxlin, E.: Inertial head-tracker sensor fusion by a complementary separate-bias Kalman filter. In: Proceedings of the IEEE 1996 Virtual Reality Annual International Symposium, Santa Clara, CA, pp. 185–194. IEEE (1996)
69. You, S., Neumann, U.: Fusion of vision and gyro tracking for robust augmented reality registration. In: Proceedings IEEE Virtual Reality 2001, Yokohama, Japan, pp. 71–78. IEEE (2001)

70. Lee, H.J., Jung, S.: Gyro sensor drift compensation by Kalman filter to control a mobile inverted pendulum robot system. In: 2009 IEEE International Conference on Industrial Technology, Gippsland, VIC, Australia, pp. 1–6. IEEE (2009)
71. Rigatos, G., Tzafestas, S.: Extended Kalman filtering for fuzzy modelling and multi-sensor fusion. Math. Comput. Model. Dyn. Syst. **13**(3), 251–266 (2007)
72. Lu, M.-L., Waters, T., Werren, D., Piacitelli, L.: Human posture simulation to assess cumulative spinal load due to manual lifting. Part II: accuracy and precision. Theor. Issues Ergon. Sci. **12**(2), 189–203 (2011)
73. Faber, G.S., Kingma, I., Bruijin, S.M., van Dieen, J.H.: Optimal inertial sensor location for ambulatory measurement of trunk inclination. J. Biomech. **42**(14), 2406–2409 (2009)